OPEN

Experimental & Molecular Medicine (2015) 47, e172; doi:10.1038/emm.2015.39

www.nature.com/emm

ORIGINAL ARTICLE

MicroRNA-103a-3p controls proliferation and osteogenic differentiation of human adipose tissue-derived stromal cells

Da Sol Kim[1], Sun Young Lee[1], Jung Hee Lee[1], Yong Chan Bae[2] and Jin Sup Jung[1]

The elucidation of the molecular mechanisms underlying the differentiation and proliferation of human adipose tissue-derived stromal cells (hADSCs) represents a critical step in the development of hADSCs-based cellular therapies. To examine the role of the microRNA-103a-3p (miR-103a-3p) in hADSCs functions, miR-103a-3p mimics were transfected into hADSCs in order to overexpress miR-103a-3p. Osteogenic differentiation was induced for 14 days in an osetogenic differentiation medium and assessed by using an Alizarin Red S stain. The regulation of the expression of *CDK6* (cyclin-dependent kinase 6), a predicted target of miR-103a-3p, was determined by western blot, real-time PCR and luciferase reporter assays. Overexpression of miR-103a-3p inhibited the proliferation and osteogenic differentiation of hADSCs. In addition, it downregulated protein and mRNA levels of predicted target of miR-103a-3p (*CDK*6 and *DICER1*). In contrast, inhibition of miR-103a-3p with 2′O methyl antisense RNA increased the proliferation and osteogenic differentiation of hADSCs. The luciferase reporter activity of the construct containing the miR-103a-3p target site within the *CDK6* and *DICER1* 3′-untranslated regions was lower in miR-103a-3p-transfected hADSCs than in control miRNA-transfected hADSCs. RNA interference-mediated downregulation of *CDK6* and *DICER1* in hADSCs inhibited their proliferation and osteogenic differentiation. The results of the current study indicate that miR-103a-3p regulates the osteogenic differentiation of hADSCs and proliferation of hADSCs by direct targeting of *CDK6* and *DICER1* partly. These findings further elucidate the molecular mechanisms governing the differentiation and proliferation of hADSCs.
Experimental & Molecular Medicine (2015) **47,** e172; doi:10.1038/emm.2015.39; published online 10 July 2015

INTRODUCTION

MicroRNAs (miRNAs) are endogenous 19- to 25-nucleotide non-coding RNAs that bind to partially complementary recognition sequences of mRNA, resulting in translational repression or cleavage and degradation of mRNA, thus regulating the expression of mRNA targets.[1] Each miRNA can regulate multiple mRNAs and each mRNA can be targeted by a number of miRNAs. Thus, it has been estimated that as many as 30% of protein-coding genes could be targets of miRNAs. miRNAs have been shown to be involved in diverse biological processes including cellular differentiation,[2] proliferation,[3] apoptosis[4] and metabolism.[5] miRNAs also have important roles in the self-renewal and pluripotency of stem cells.[6,7] The functions of one particular miRNA, miR-103a, have been investigated in several cancer cell lines. For example, the expression of miR-103 was found to be decreased in papillary thyroid cancer cells,[8] but increased in endometrial cancer,[9] nasopharyngeal carcinoma,[10] pancreatic cancer,[11] bladder cancer,[12] colorectal cancer[4] and lung cancer cells.[13] In colorectal cancer cells, miR-103 was found to target a gene that induces apoptosis of cancer cells (*PER3*),[4] and the tumor suppressor genes *DICER* and *PTEN*.[14] In studies that examined the effects of miR-103 on cellular differentiation and proliferation, silencing of miR-103 decreased total fat by reducing adipocyte size,[15] and inhibited proliferation of mouse intestinal cell by targeting the *CCNE1*, *CDK2*, and *CREB1* genes.[16] Bioinformatic studies have predicted a role for miR-103/miR-107 paralogs in lipid and energy metabolism with a prediction that miR-103/107 regulates human metabolic pathways.[17]

Adipose tissue, like bone marrow, is a mesodermally derived organ with a stromal cell population. This population, termed adipose tissue-derived mesenchymal stem cells or adipose tissue stromal cells (ADSCs), shares many of its characteristics

[1]Department of Physiology, School of Medicine, Pusan National University, Yangsan, Korea and [2]Department of Plastic Surgery, School of Medicine, Pusan National University, Pusan, Korea
Correspondence: Professor JS Jung, Department of Physiology, School of Medicine, Pusan National University, Beomeo-ri, Mulgeum-eup, Yangsan-si 626-870, Gyeongsangnam-do, Korea.
E-mail: jsjung@pusan.ac.kr
Received 21 November 2014; revised 3 March 2015; accepted 10 March 2015

with bone marrow, including extensive proliferative potential and the ability to differentiate toward adipogenic, osteogenic, chondrogenic and myogenic lineages. Elucidating the molecular events involved in adipocyte differentiation is necessary in order to develop trapeutics for metabolic diseases such as obesity and diabetes.[18] Toward that end, our laboratory has reported that several miRNAs control proliferation and differentiation of human ADSCs (hADSCs).[19–21]

In the current study, we examined the role of miR-103a-3p on the proliferation and osteogenic differentiation of hADSCs. The data in this study suggested that miR-103a-3p inhibited hADSCs proliferation and osteogenic differentiation by binding to specific target sequences in the -*CDK6* mRNA 3′-untranslated region (UTR).

MATERIALS AND METHODS

Cell culture

All protocols involving human subjects were approved by the Institutional Review Board of Pusan National University. Superfluous materials were collected from four individuals undergoing elective abdominoplasty after informed consent was given by each individual. We isolated the hADSCs according to the methods which described in previous studies.[22] The hADSCs were maintained in α-minimal essential medium (MEM) with 10% fetal bovine serum, 100 μg ml^{-1} streptomycin and 100 mg ml^{-1} penicillin in 5% CO_2 environment at 37 °C.

Osteogenic differentiation

Osteogenic differentiation was induced through the culturing of the cells for 10 days–2 weeks in osteogenic medium (10% fetal bovine serum, 0.1 mM dexamethasone, 10 mM β-glycerophosphate, and 50 mM ascorbic acid in α-MEM), and extracellular matrix calcification was estimated by using 2% Alizarin Red S with a pH of 4.3 (Sigma-Aldrich, St Louis, MO, USA) for 15 min. For obtaining quantitative data, 300 μl of 10% (w/v) cetylpyridinium chloride (Sigma-Aldrich) and 10 mM sodium phosphate (pH 7.0) solution was added to stained dishes and the absorbance of extracted dye was determined at 562 nm.

Evaluation of cell proliferation

hADSCs were transfected with miRNA or small interfering RNA (siRNA). After a 48 h incubation, the cells were detached and the plated in 6-well plates at a density of 1×10^4 cells per well. The number of cells was counted at the indicated days after plating with a Countess Automated Cell Counter (Invitrogen, Carlsbad, CA, USA).

Real-time quantitative PCR

Total RNA was isolated by using Trizol (Invitrogen), according to the manufacturer's instructions and reverse-transcribed into cDNA with the Reverse Transcriptase M-MLV (Promega, Madison, WI, USA). Primer sequences to be used in the experiment were as follows: *CDK6*: FW: 5′-TCACACCGAGTAGTGCATCG-3′, RV: 5′-CAAGACTTCGG GTGCTCTGT-3′; *Runx2*: FW: 5′-CTCACTACCACACCTACCTG-3′, RV: 5′-TCAATATGGTCGCCAAACAGATTC-3′; *Alkaline phosphatase*: FW: 5′-CCACGTCTTCACATTTGGTG-3′, RV: 5′-AGACTGCG CCTGGTAGTTGT-3′. For miRNA quantitative reverse transcriptase PCR, small RNA species-enriched RNA was isolated according to the manufacturer's instructions (mirVana miRNA isolation kit; Ambion, Austin, TX, USA). miRNA was reverse-transcribed by using Ncode miRNA first-strand complementary DNA synthesis kits (Invitrogen). Forward primer sequence was designed as the corresponding mature miRNA sequences and 5S ribosomal RNA was used as normalizing control. The miR-103a-3p-specific forward primer sequence was designed on the basis of miRNA sequences obtained from the miRBase database. Quantitative reverse transcriptase PCR was performed by using a Power SYBR Green PCR Master Mix on the ABI7500 Instrument (Applied Biosystems, Warrington, UK). Data analysis was determined by using the relative standard curve method.

Western blot analysis

Samples were homogenized in RIPA buffer (Sigma, St Louis, MO, USA). The isolated proteins were separated by SDS-PAGE and electrotransferred to Nitrocellulose membranes (Millipore, Bedford, MA, USA). Blots were probed with primary antibodies, followed by horseradish peroxidase-conjugated secondary antibodies. Antibodies used in this study were purchased as follows: *CDK6* from Abcam (Cambridge, UK), *DICER1* from Santa Cruz Biotechnology (Santa Cruz, CA, USA) and GAPDH from Cell Signaling Technologies (Boston, MA, USA). Bound antibodies were detected by using an ECL detection kit (Pierce Biotechnology, Rockford, IL, USA) and visualized by using LAS 3000 Luminoimage Analyzer (Fujifilm, Tokyo, Japan). Protein level was quantified by using the National Institutes of Health ImageJ software (Bethesda, MD, USA).

miRNA/siRNA transfection

hADSCs were seeded with complete medium without antibiotics. On the following day, 20 nM of miRNAs (miR-103a-3p mimics or inhibitors, Dharmacon, Thermo Scientific, Epsom, UK) and 100 nM of siRNAs (on-TARGET plus SMART pool, Dharmacon) for *CDK6* and *DICER1* were transfected by using DharmaFECT Transfection Reagent I (Dharmacon) according to manufacturer's protocol. As negative control, control miRNA or non-targeting siRNA were transfected.

Reporter vectors and DNA consturcts

Putative miR-103a-3p-recognition elements (as single copy) from the *CDK6* gene and *DICER1* were cloned in the 3′-UTR of the firefly luciferase reporter vector (pMIR-Report, Ambion) according to the manufacturer's specified guidelines. The oligonucleotide sequences were designed to carry the *HindIII* and *SpeI* sites at their extremities facilitating ligation into the *HindIII* and *SpeI* sites of pMIR-Report (Ambion). The oligonucleotides used in these studies were as follows:

pMIR-*CDK6* FW:5′-CTAGTAAAAAGATTGGAACTGTTACGAC GGA-3′,

RV: 5′-AGCTTCCGTCGTAACAGTTCCAATCTTTTTA-3′

pMIR-*CDK6* mutant FW: 5′-CTACTAAAAAGATTGAAACTG TTCCGTTGGA-3′,

RV: 5′-AGCTTCCAACGGAACAGTTTCAATCTTTTTA-3′

pMIR-*DICER1* FW: 5′-CTAGTATAGTGTGGATTTTATACGAC GTA-3′,

RV: 5′-AGCTT ACGTCGTATAAAATCCACACTATA-3′,

pMIR-*DICER1* mutant FW: 5′-CTAGTATAGTGTGGATTTCA CAAGACGTA-3′,

RV: 5′-AGCTT ACGTCTTGTGAAATCCACACTATA-3′

Reporter gene assay

All transient transfections were conducted by using Dharmafect Duo (Dharmacon, Thermo Scientific). The pMIR-*CDK6* and pMIR-β-gal plasmids were used as reporter constructs. The cells were harvested 72 h after transfection, lysed in reporter lysis buffer, and subsequently

assayed for their luciferase activity (Luciferase Assay System, Promega). The transfections were performed in duplicate per each experiment. The luciferase assays were normalized according to their β-galactosidase activity.

Stastistical analysis

All of the results are presented as the means ± s.e.m. Comparisons between groups were analyzed via *t*-tests (two-sided) or analysis of variance for experiments with more than two subgroups. *Post hoc* range tests and pair-wise multiple comparisons were conducted by using the *t*-test (two-sided) with Bonferroni adjustments. Probability values of $P<0.05$ were considered to be statistically significant.

RESULTS

Effects of miR-103a-3p overexpression on the osteogenic differentiation and proliferation of hADSCs

The miRNAs that showed high levels of expression in a preliminary miRNA microarray study were chosen and then differentiation-related molecules were targeted by using the miRWalk database.[23] To examine the role of miR-103a-3p in hADSCs functions, miR-103a-3p mimics were transfected into hADSCs in order to overexpress miR-103a-3p. miRNA mimics augment the function of endogenous miRNAs for easier detection of phenotypic changes. Real-time PCR analysis showed that miR-103a-3p-transfected hADSCs had increased levels of miR-103a-3p expression (Figure 1a).

To test the effect of miR-103a-3p on hADSCs proliferation, miR-103a-3p-transfected hADSCs were plated (1×10^4 cells per well) on culture plates and the number of cells was counted on specific days. This cell counting experiment showed that miR-103a-3p-transfected cells had slower growth than control miR-transfected cells (Figure 1b). Osteogenic differentiation of miR-103a-3p-overexpressing hADSCs were induced with the appropriate media. After incubating hADSCs for 14 days after inducing differentiation, miR-103a-3p-overexpression significantly inhibited an osteogenic differentiation of hADSCs (Figure 1c). Real-time PCR analysis showed that the transfection of a miR-103a-3p mimic inhibited alkaline phosphatase expression at basal and 7 days after osteogenic differentiation (Figure 1d).

Effects of miR-103a-3p inhibition on the osteogenic differentiation and proliferation of hADSCs

To investigate the effect of miR-103a-3p inhibition on hADSCs differentiation, hADSCs were transfected with a specific miRNA inhibitor (IH-miR-103a-3p). Real-time PCR analysis showed that transfection of IH-miR-103a-3p effectively down-regulated miR-103a-3p expression in hADSCs (Figure 2a).

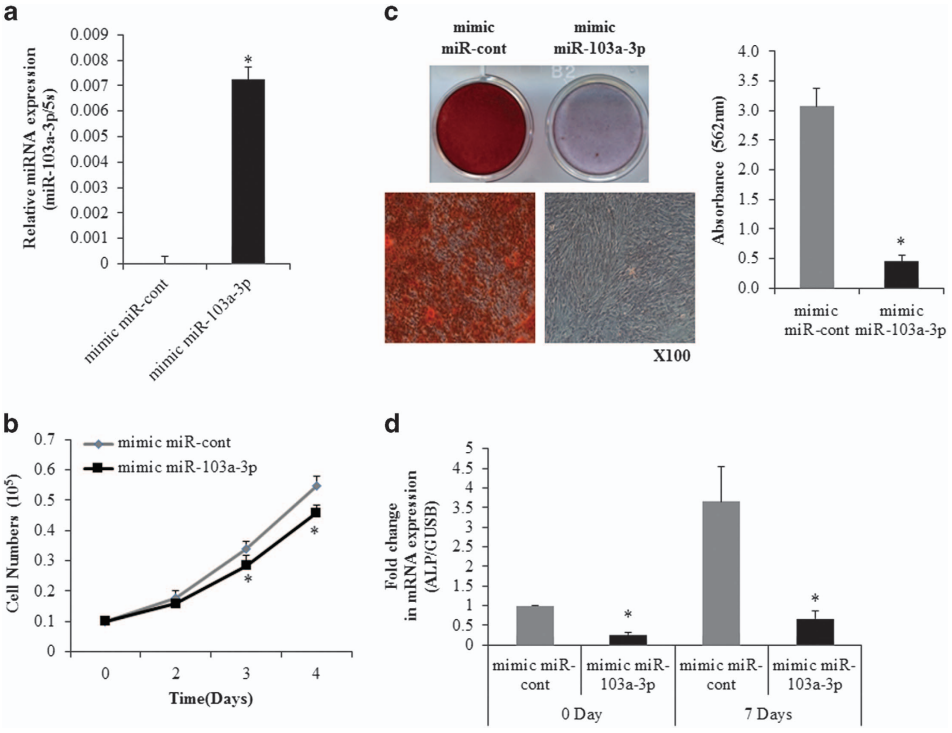

Figure 1 Overexpression of miR-103a-3p inhibits osteogenic differentiation and proliferation of hADSCs. (**a**) miR-103a-3p levels were determined in mimic control (mimic miR-cont) or mimic miR-103a-3p-transfected hADSCs using real-time PCR. (**b**) hADSCs proliferation was determined by direct cell counting after oligonucleotide transfection. (**c**) Oligonucleotide-transfected hADSCs were grown for 2 days and, when the oligonucleotide-transfected hADSCs were grown to 80–90% confluence, osteogenic differentiation was induced for 2 weeks and determined by Alizarin Red S solution, which was quantified by absorbance at 562 nm. (**d**) Real-time PCR analysis of ALP, in mimic miR-103a-3p-transfected undifferentiated and differentiated cells. Total RNA was isolated at days after induction of differentiation. Internal control for expression analysis was GUSB. Data represent mean ± s.e.m. ($n=4$). *$P<0.05$ compared with mimic miR-cont-transfected hADSCs at 0 and 7 days. ALP, alkaline phosphatase; hADSC, human adipose tissue-derived stromal cell; miR, microRNA.

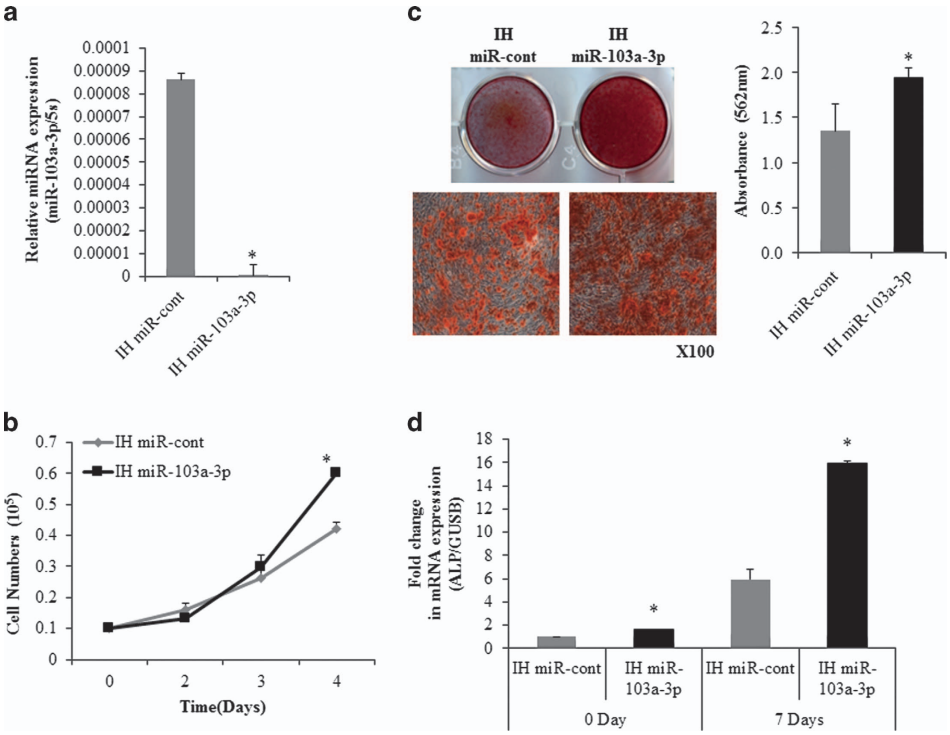

Figure 2 Inhibition of miR-103a-3p increases osteogenic differentiation and proliferation of hADSCs. (**a**) miR-103a-3p levels were determined in inhibitor control-(IH-miR-cont) or IH-miR-103a-3p–transfected hADSCs using real-time PCR. (**b**) hADSCs proliferation was determined by direct cell counting after oligonucleotide transfection. (**c**) Oligonucleotide-transfected hADSCs were grown for 10 days and, when the oligonucleotide-transfected hADSCs were grown to 80–90% confluence, osteogenic differentiation was induced for 2 weeks and determined by Alizarin Red S solution staining, which was quantified by absorbance at 562 nm. (**d**) Real-time PCR analysis of ALP in IH-miR-103a-3p-transfeted undifferentiated and differentiated cells. Total RNA was isolated at days after induction of differentiation. Internal control for expression analysis was GUSB. Data represent mean ± s.e.m. ($n=4$). *$P<0.05$ compared with IH-miR-cont transfected hADSCs at 0 and 7 days. ALP, alkaline phosphatase; hADSC, human adipose tissue-derived stromal cell; miR, microRNA.

The cell counting experiment showed that IH-miR-103a-3p enhanced hADSCs proliferation compared with control oligonucleotide-transfected cells (Figure 2b).

To examine the effect of miR-103a-3p inhibition on osteogenic differentiation, IH-miR-103a-3p-transfected hADSCs were induced to differentiate into osteogenic lineages. Alizarin Red S staining revealed that the inhibition of miR-103a-3p enhanced an osteogenic differentiation of hADSCs (Figure 2c). To further confirm the effect, the expression of osteogenic differentiation marker gene was determined using real-time PCR. Results showed that IH-miR-103a-3p transfection increased the expression of alkaline phosphatase at basal and 7 days after osteogenic differentiation (Figure 2d).

miR-103a-3p targets the 3′-UTR of *CDK6* mRNA

To determine the potential targets of miR-103a-3p in hADSCs, miR-103a-3p-induced changes in gene expression profiles were analyzed by microarray. The transfection of a miR-103a-3p mimic lead to increased the expression of 32 genes and inhibited the expression of 31 genes in hADSCs (Table 1). Using the miRWalk database for target gene prediction, *CDK6* was selected as a potential target of miR-103a-3p among the downregulated genes.

To determine the relationship between miR-103a-3p and *CDK6*, *CDK6* expression was analyzed with real-time PCR and western blot analysis in miR-103a-3p mimic transfected cells. The transfection of a mimic miR-103a-3p led to a significant decrease in *CDK6* protein (Figure 3a) and mRNA (Figure 3b) expression levels in the hADSCs.

To test whether miR-103a-3p directly targeted *CDK6* in hADSCs, luciferase reporter genes with *CDK6* 3′-UTRs with or without mutation at the miR-103a-3p binding regions were constructed (Figure 3c). The results showed a decrease in relative luciferase activity when the *CDK6* 3′-UTR (pMIR-*CDK6*) was transfected into miR-103a-3p-transfected hADSCs, while no decrease in relative luciferase activity was observed in hADSCs transfected with a mutant miR-103a-3p 3′-UTR (pMIR-*CDK6*-mut) (Figure 3d).

Effect of *CDK6* siRNA on proliferation and osteogenic differentiation of hADSCs

To determine the role of *CDK6* in osteogenic differentiation and proliferation of hADSCs, *CDK6* expression was suppressed in hADSCs with an RNA interference technique using *CDK6*

Table 1 Partial list of genes of which expression are regulated by miR-103a-3p-overexpress hADSCs

Gene symbol	*Gene name*	*Fold change*
SMPD1	Sphingomyelin phosphodiesterase 1	−6.55
CDK6	Cyclin-dependent kinase 6	−5.63
MT1M	Metallothionein 1 M	−4.23
UNC84B	Sad1 and UNC84 domain containing 2	−3.67
MT1E	Metallothionein 1E	−3.13
GREM2	Gremlin 2, DAN family BMP antagonist	−2.90
DICER1	Ribonuclease type III	−2.87
TRIAP1	TP53 regulated inhibitor of apoptosis 1	−2.87
VCAM1	Vascular cell adhesion molecule 1	−2.86
GRN	Granulin	−2.70
CUL4A	Cullin 4A	−2.60
UBE2C	Ubiquitin-conjugating enzyme E2C	−2.50
S1PR3	Suppression of tumorigenicity 13	−2.35
BIRC5	Baculoviral IAP repeat containing 5	−2.30
IL6	Interleukin 6	−2.24
IL13RA1	Interleukin 13 receptor, alpha 1	3.27
ARNT2	Aryl-hydrocarbon receptor nuclear translocator 2	3.22
UBE2G1	Ubiquitin-conjugating enzyme E2G 1	3.04
CANX	Calnexin	2.98
NDUFB5	NADH dehydrogenase (ubiquinone) 1 beta subcomplex, 5	2.84
RRAS2	Related RAS viral (r-ras) oncogene homolog 2	2.81
ANKRD37	Ankyrin repeat domain 37	2.79
TPMT	Thiopurine S-methyltransferase	2.57
YWHAB	Tyrosine 3-monooxygenase/tryptophan 5-monooxygenase activation protein, beta polypeptide	2.57

Abbreviations: hADSC, human adipose tissue-derived stromal cell; miR, microRNA.

siRNA (*CDK6* siRNA) transfection. Real-time PCR analysis confirmed that *CDK6* siRNA effectively inhibited *CDK6* expression in hADSCs (Figure 4a). Direct cell counting showed that *CDK6* siRNA-transfected hADSCs proliferated less than the control cells (Figure 4b).

To study the effect of *CDK6* downregulation on the efficiency of hADSCs differentiation, osteogenic differentiation of *CDK6* siRNA-transfected hADSCs was induced. Alizarin Red S staining, and real-time PCR analysis of osteogenic differentiation marker genes indicated that downregulation of *CDK6* inhibited osteogenic differentiation of hADSCs (Figure 4c and d).

miR-103a-3p targets the 3′-UTR of *DICER1* mRNA

To determine the relationship between miR-103a-3p and *DICER1*, *DICER1* expression was analyzed with real-time PCR and western blot analysis in miR-103a-3p mimic-transfected cells. The transfection of a miR-103a-3p mimic led to a significant decrease in *DICER1* expression at both the protein (Figure 5a) and mRNA (Figure 5b) levels in the hADSCs.

To test whether miR-103a-3p directly targeted *DICER1* in hADSCs, luciferase reporter genes with *DICER1* 3′-UTRs with or without mutation at the miR-103a-3p-binding regions were constructed and the changes in luciferase activity with miR-103a-3p transfection were determined. The results showed that miR-103a-3p transfection inhibited luciferase activity in hADSCs that were transfected with the constructs containing *DICER1* 3′-UTR (pMIR-*DICER1*) or mutant miR-103a-3p 3′-UTR (pMIR-*DICER1*-mut; Figure 5c and d).

Effect of *DICER1* on osteogenic differentiation and proliferation of hADSCs

To determine the role of *DICER1* in osteogenic differentiation and proliferation of hADSCs, *DICER1* expression was suppressed in hADSCs with an RNA interference technique using *DICER1* siRNA (*DICER1* siRNA) transfection. Real-time PCR analysis confirmed that *DICER1* siRNA effectively inhibited *DICER1* expression in hADSCs (Figure 6a). The effect of *DICER1* downregulation on hADSCs proliferation was also determined. Direct cell counting showed that *DICER1* siRNA-transfected hADSCs proliferated less than the control cells (Figure 6b).

To study the effect of *DICER1* downregulation on the efficiency of hADSC differentiation, osteogenic differentiation of *DICER1* siRNA-transfected hADSCs was induced. Alizarin Red S staining indicated that downregulation of *DICER1* inhibited osteogenic differentiation of hADSCs (Figure 6c).

DISCUSSION

Although several reports have demonstrated the function of miR-103a in the neurogenesis of embryonic stem cells,[24] studies have not examined its effects on the differentiation of other cell lineages. In the current study, we investigated whether miR-103a-3p was involved in proliferation and osteogenic differentiation of hADSCs. The data in this study demonstrated that miR-103a-3p overexpression with its mimic in hADSCs inhibited proliferation and osteogenic differentiation, and that miR-103 inhibition by transfection of inhibitor oligonucleotides increased osteogenic differentiation and proliferation. These results indicated that miR-103-3p was a negative regulator of osteogenic differentiation and proliferation in hADSCs.

Downregulated genes in miR-103a-3p mimic-transfected cells, including *CDK6* was identified from a microarray experiment. The data from the current experiment showed that overexpression of miR-103 downregulated the expression of *CDK6* at the protein and mRNA levels. An assay with a firefly luciferase reporter plasmid containing the predicted *CDK*6 target gene sequences showed that overexpression of miR-103 decreased luciferase activity, confirming the direct binding of miR-103 to the 3′-UTRs of *CDK6* in hADSCs. Roles for *CDK6* in the miR-103a-induced inhibition of the proliferation and osteogenic differentiation of hADSCs was further supported by determining the effects of *CDK6* siRNAs. Downregulation of *CDK6* showed similar changes in the phenotypes of hADSCs with miR-103a overexpression.

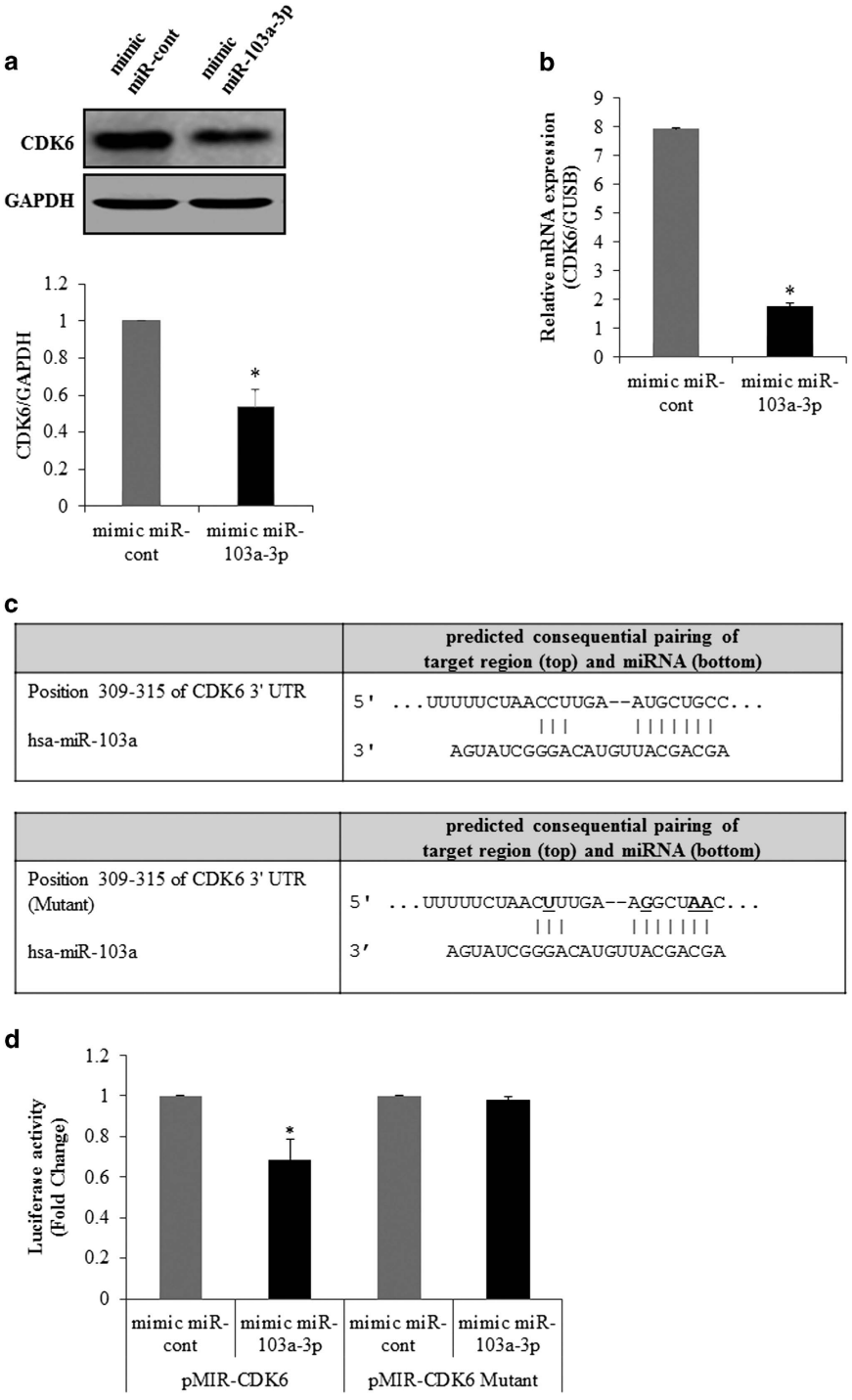

Figure 3 miR-103a-3p targets the 3′-UTR of *CDK6* mRNA. (**a**) *CDK6* expression in hADSCs transfected with oligonucleotides was analyzed by western blot. Lysates were prepared at 2 days after transfection with oligonucleotides. To confirm equal loading, the quantities of *CDK6* and GAPDH were determined using anti-*CDK6* and anti-GAPDH antibodies. The relative expression ratio of each protein was quantified by densitometric evaluation of western blots. Data represent mean ± s.e.m. ($n=4$). *$P<0.05$ compared with mimic-miR-cont transfected hADSCs. (**b**) *CDK6* expression in hADSCs transfected with oligonucleotides was analyzed by real-time PCR. Total RNAs were isolated at 2 days after transfection with oligonucleotides. Data represent mean ± s.e.m. ($n=4$). *$P<0.05$ compared with mimic-miR-cont transfected hADSCs. (**c**) pMIR-*CDK6* or pMIR-*CDK6*-mutant luciferase constructs were made according to the sequences from miRWalk database. (**d**) These contructs were cotransfected with mimic-miR-103a-3p or mimic-miR-control into hADSC. Data represent mean ± s.e.m. of the ratio to the value of mimic miR-cont of pMIR-*CDK6* or pMIR-*CDK6* mutant ($n=4$), *$P<0.05$ compared with mimic miR-cont-transfected hADSCs. hADSC, human adipose tissue-derived stromal cell; miR, microRNA; UTR, untranslated region.

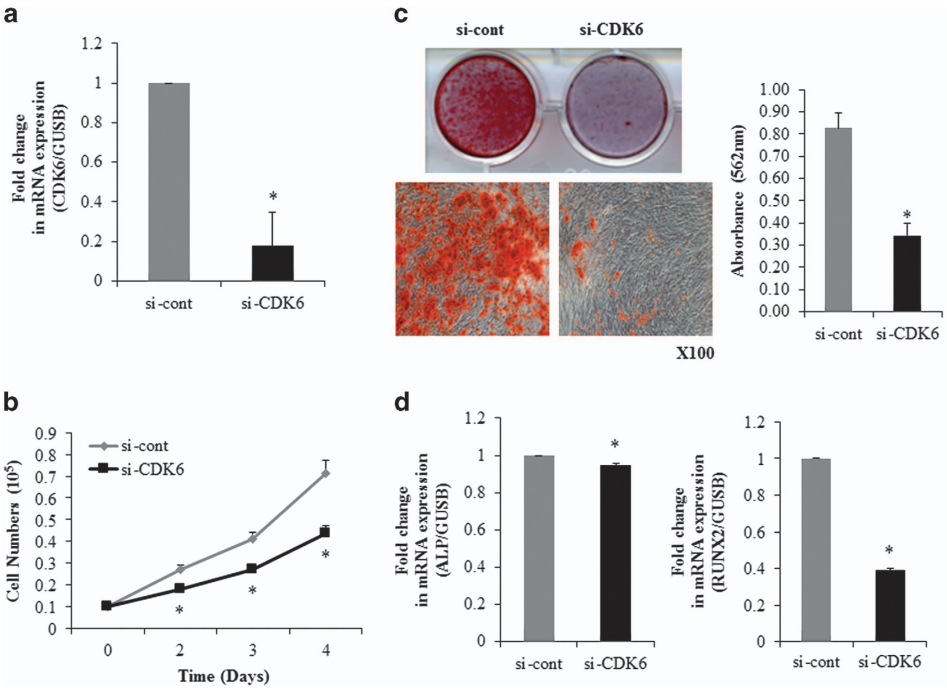

Figure 4 *CDK6* siRNA inhibits osteogenic differentiation and proliferation of hADSCs. (**a**) *CDK6* mRNA levels were determined in control- (si-cont) or *CDK6* oligonucleotide (si-*CDK6*) transfected hADSCs by using real-time PCR. Internal control for expression analysis was GUSB. (**b**) hADSCs proliferation was determined by direct cell counting. (**c**) Oligonucleotide-transfected hADSCs were grown for 2 days and, when the oligonucleotide-transfected hADSCs were grown to 80–90% confluence, osteogenic differentiation was induced for 2 weeks and determined by Alizarin Red S solution staining, which was quantified by absorbance at 562 nm. (**d**) Real-time PCR analysis of ALP, and Runx2 in si-*CDK6*-transfected undifferentiated cells. Internal control for expression analysis was GUSB. Data represent mean ± s.e.m. ($n=4$). $^*P<0.05$ compared with si-cont-transfected hADSCs. ALP, alkaline phosphatase; hADSC, human adipose tissue-derived stromal cell; miR, microRNA; si-*CDK6*, *CDK6* small interfering RNA.

CDK6 was identified as a new member in a family of cdc-2 related kinases in 1992.[25] This kinase, which is a partner with the D-type cyclins and possesses pRb kinase activity *in vitro*, has been thought to function solely as a pRb kinase in the regulation of the G1 phase of the cell cycle.[26] Additional research indicated that miRNA-504 inhibited hypopharyngeal squamous cell carcinoma cell proliferation via targeting *CDK6*.[27] Overexpression of *CDK6* has been shown to block differentiation of mice chondrocytes without affecting cell-cycle progression *in vitro*.[28] It has also been reported that several miRNAs target *CDK6* and control cell proliferation and osteogenic differentiation. miR-137[29] inhibits the proliferation of lung cancer cells by targeting *CDK6* and cdc42. miR-34a inhibits osteoblast differentiation and cell proliferation in human mesenchymal stem cells through the inhibition of multiple targets including *CDK6*.[30]

DICER1 is a conserved RNAse III endonuclease that is essential for the processing of several classes of small RNAs, including miRNAs and endo-siRNAs, as well as for the degradation of toxic transposable elements.[31,32] *DICER1* has an important role in the proliferation and differentiation of oligodendrocyte precursor cells and in the development of pancreatic endocrine cells.[33] Oskowitz *et al.*[34] reported that downregulation of Dicer expression did not affect cell proliferation in human bone marrow-derived mesenchymal stem cells, a finding which is inconsistent with data from the current study. *DICER1* deletion has various effects on cell proliferation. Silencing of *DICER1* inhibited cell proliferation in leukemia cells,[35] however, a decrease in *DICER1* expression by miR-192 increased proliferation of neuroblastoma cells.[36] Therefore, the effects of *DICER1*on cell proliferation may differ based on the miRNA profiles present in different cell types.

Conditional deletion of the Dicer enzyme in osteoprogenitors by Col1a1-Cre compromised fetal survival after E14.5 and demonstrated impaired extracellular matrix mineralization and reduced expression of mature osteoblast markers during differentiation of mesenchymal cells of *ex vivo* deleted Dicer (c/c).[37] This supports our findings that downregulation of *DICER1* expression inhibits osteogenic differentiation of hADSCs.

In this study microarray data showed that miR-103a-3p downregulated 31 genes. It has been known that interleukin 6[38] and gemlin 2[39] inhibited osteoblast differentiation. Therefore, these genes could be excluded potential targets of miR-103a-3p. However, we cannot exclude the possibility that other genes besides of *CDK6* may be involved in the miR-103-induced inhibition of osteogenic differentiation in hADSCs.

Collectively, the findings from the current study indicate that miR-103a controls the proliferation and osteogenic differentiation of hADSCs, and that these effects are partly mediated by

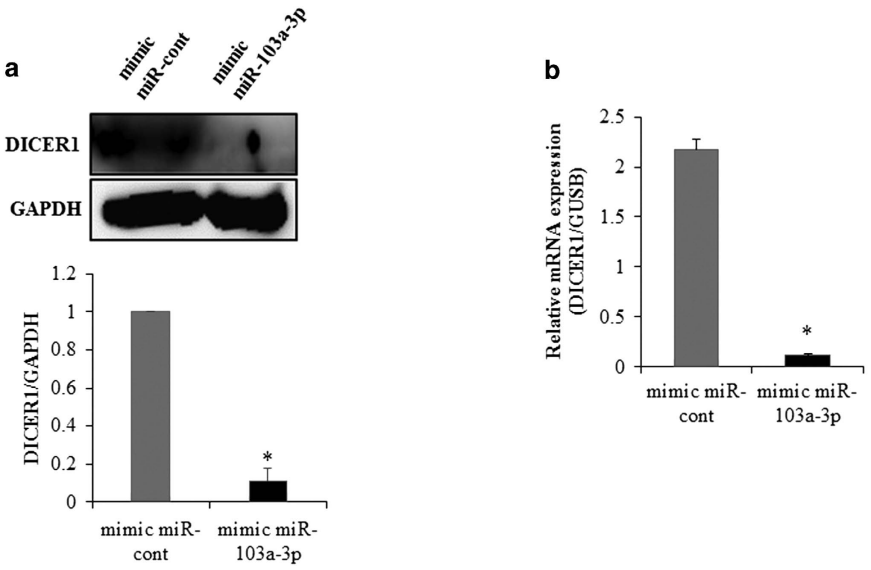

c

	predicted consequential pairing of target region (top) and miRNA (bottom)
Position 1150-1157 of *DICER1* 3' UTR hsa-miR-103a	5' ... UAUCACACCUAAAAUAUGCUGCA... 3' ACUAUCGGGACAUGUUACGACGA

	predicted consequential pairing of target region (top) and miRNA (bottom)
Position 1150-1157 of *DICER1* 3' UTR (Mutant) hsa-miR-103a	5' ... UAUCACACCUAAAAUAUGCUGCA... 3' ACUAUCGGGACAUGUUACGACGA

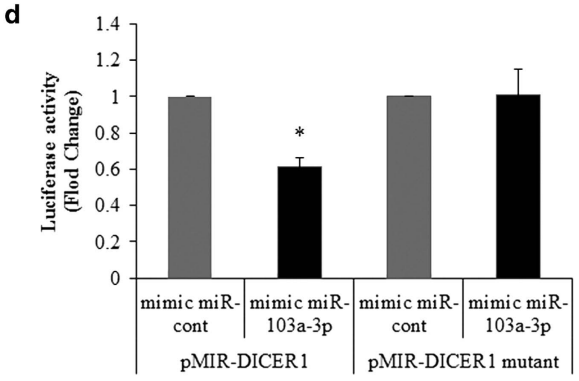

Figure 5 miR-103a-3p targets the 3′-UTR of *DICER1* mRNA. (**a**) *DICER1* expression in hADSCs transfected with oligonucleotides was analyzed by western blot. Lysates were prepared at 2 days after transfection with oligonucleotides. To confirm equal loading, the quantities of *DICER1* and GAPDH were determined using anti-*DICER1* and anti-GAPDH antibodies. The relative expression ratio of each protein was quantified by densitometric evaluation of western blots. Data represent mean ± s.e.m. ($n=4$). *$P<0.05$ compared with mimic-miR-cont transfected hADSCs. (**b**) *DICER1* expression in hADSCs transfected with oligonucleotides was analyzed by real-time PCR. Total RNAs were isolated at 2 days after transfection with oligonucleotides. Data represent mean ± s.e.m. ($n=4$). *$P<0.05$ compared with mimic-miR-cont transfected hADSCs. (**c**) pMIR-*DICER1* or pMIR-*DICER1*-mutant luciferase constructs were made according to the sequences from miRWalk database. (**d**) pMIR-*DICER1* or pMIR-*DICER1*-mutant luciferase constructs were cotransfected with mimic-miR-103a-3p or mimic-miR-control into hADSCs hADSCs. Internal control for expression analysis was *GUSB*. Data represent mean ± s.e.m. of the ratio to the value of mimic miR-cont of pMIR-*DICER1* or pMIR-*DICER1* mutant ($n=4$), *$P<0.05$ compared with miR-con-transfected hADSCs, #$P<0.05$ compared with anti-miR-cont-transfected hADSCs. hADSC, human adipose tissue-derived stromal cell; miR, microRNA; UTR, untranslated region.

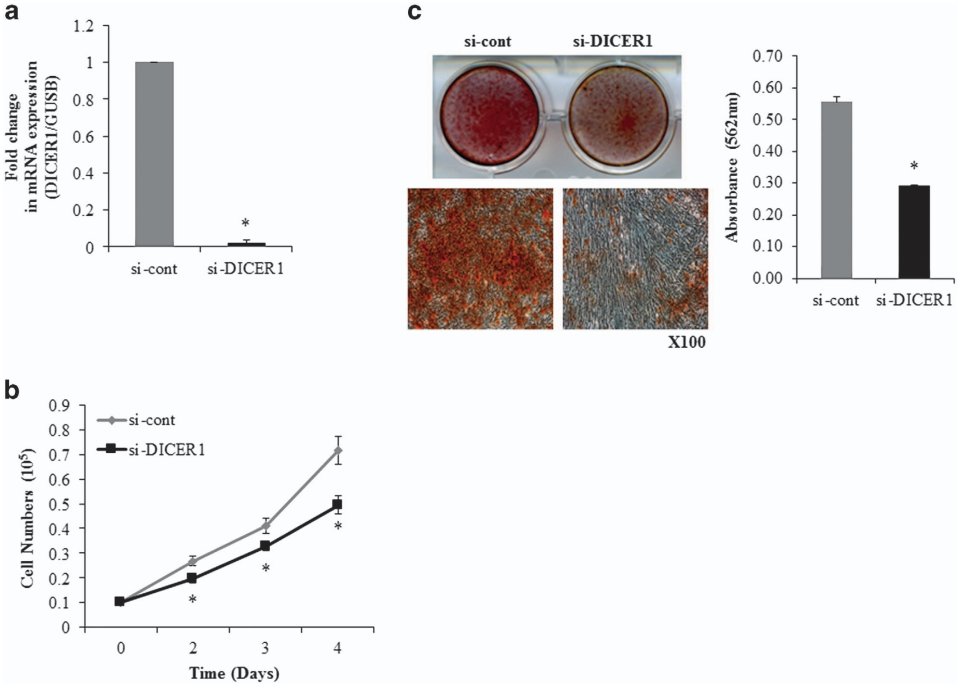

Figure 6 *DICER1* RNAi inhibits osteogenic differentiation and proliferation of hADSCs. (**a**) *DICER1* mRNA levels were determined in control-(si-cont) or *DICER1* oligonucleotide-(si-*DICER1*) transfected hADSCs by using real-time PCR. (**b**) hADSCs proliferation was determined by direct cell counting. (**c**) Osteogenic differentiation were determined same as Figure 1c method. Data represent mean ± s.e.m. ($n=4$). *$P<0.05$ compared with si-con-transfected hADSCs. hADSC, human adipose tissue-derived stromal cell; si-*DICER1*, *DICER1* small interfering RNA.

targeting the 3′-UTRs of *CDK6*. These results are important, as novel pharmacological agents for disease treatment based on targeting miRNAs are already undergoing clinical trials.[40] Previous studies in mice have shown that targeting miRNA led to the development of osteoporotic bone in mice[41] and contributed to primary osteoporosis in humans.[42,43] Thus, inhibition of miR-103a in mesenchymal stem cells *in vivo* may lead to enhanced bone formation. It is plausible that local implantation of human mesenchymal stem cells cultured on a functionalized scaffold containing IH-miR-103a may represent one approach to enhance local bone formation needed for treatment of localized bone defects and non-healed fractures.

CONFLICT OF INTEREST

The authors declare no conflict of interest.

ACKNOWLEDGEMENTS

This research was supported by the National Research Foundation of Korea (NRF) funded by the Ministry of Science, ICT and Future Planning (NRF-2012M3A9B4028558).

1 Huntzinger E, Izaurralde E. Gene silencing by microRNAs: contributions of translational repression and mRNA decay. *Nat Rev Genet* 2011; **12**: 99–110.
2 Shi XE, Li YF, Jia L, Ji HL, Song ZY, Cheng J *et al.* MicroRNA-199a-5p affects porcine preadipocyte proliferation and differentiation. *Int J Mol Sci* 2014; **15**: 8526–8538.
3 Schober A, Nazari-Jahantigh M, Wei YY, Bidzhekov K, Gremse F, Grommes J *et al.* MicroRNA-126-5p promotes endothelial proliferation and limits atherosclerosis by suppressing Dlk1. *Nat Med* 2014; **20**: 368–376.
4 Hong Z, Feng Z, Sai Z, Tao S. PER3, a novel target of miR-103, plays a suppressive role in colorectal cancer *in vitro*. *BMB Rep* 2014; **47**: 500–505.
5 Ukai T, Sato M, Akutsu H, Umezawa A, Mochida J. MicroRNA-199a-3p, microRNA-193b, and microRNA-320c are correlated to aging and regulate human cartilage metabolism. *J Orthop Res* 2012; **30**: 1915–1922.
6 Cairo S, Wang Y, de Reynies A, Duroure K, Dahan J, Redon MJ *et al.* Stem cell-like micro-RNA signature driven by Myc in aggressive liver cancer. *Proc Natl Acad Sci USA* 2010; **107**: 20471–20476.
7 Liu T, Chen Q, Huang Y, Huang Q, Jiang L, Guo L. Low microRNA-199a expression in human amniotic epithelial cell feeder layers maintains human-induced pluripotent stem cell pluripotency via increased leukemia inhibitory factor expression. *Acta Biochim Biophys Sin (Shanghai)* 2012; **44**: 197–206.
8 Liu X, He M, Hou Y, Liang B, Zhao L, Ma S *et al.* Expression profiles of microRNAs and their target genes in papillary thyroid carcinoma. *Oncol Rep* 2013; **29**: 1415–1420.
9 Boren T, Xiong Y, Hakam A, Wenham R, Apte S, Wei Z *et al.* MicroRNAs and their target messenger RNAs associated with endometrial carcinogenesis. *Gynecol Oncol* 2008; **110**: 206–215.
10 Wang HY, Yan LX, Shao Q, Fu S, Zhang ZC, Ye W *et al.* Profiling plasma microRNA in nasopharyngeal carcinoma with deep sequencing. *Clin Chem* 2014; **60**: 773–782.
11 Chakraborty C, George Priya Doss C, Bandyopadhyay S. miRNAs in insulin resistance and diabetes-associated pancreatic cancer: the 'minute and miracle' molecule moving as a monitor in the 'genomic galaxy'. *Curr Drug Targets* 2013; **14**: 1110–1117.
12 Scheffer AR, Holdenrieder S, Kristiansen G, von Ruecker A, Muller SC, Ellinger J. Circulating microRNAs in serum: novel biomarkers for patients with bladder cancer? *World J Urol* 2014; **32**: 353–358.
13 Zhu X, Zhang X, Wang H, Song Q, Zhang G, Yang L *et al.* MTA1 gene silencing inhibits invasion and alters the microRNA expression profile of human lung cancer cells. *Oncol Rep* 2012; **28**: 218–224.

14 Geng L, Sun B, Gao B, Wang Z, Quan C, Wei F *et al.* MicroRNA-103 promotes colorectal cancer by targeting tumor suppressor DICER and PTEN. *Int J Mol Sci* 2014; **15**: 8458–8472.
15 Trajkovski M, Hausser J, Soutschek J, Bhat B, Akin A, Zavolan M *et al.* MicroRNAs 103 and 107 regulate insulin sensitivity. *Nature* 2011; **474**: 649–653.
16 Liao Y, Lonnerdal B. Global microRNA characterization reveals that miR-103 is involved in IGF-1 stimulated mouse intestinal cell proliferation. *PLoS One* 2010; **5**: e12976.
17 Wilfred BR, Wang WX, Nelson PT. Energizing miRNA research: a review of the role of miRNAs in lipid metabolism, with a prediction that miR-103-/107 regulates human metabolic pathways. *Mol Genet Metab* 2007; **91**: 209–217.
18 Zuk P. Adipose-derived stem cells in tissue regeneration: a review. *ISRN Stem Cells* 2013; **2013**: 1–35.
19 Shin KK, Kim YS, Kim JY, Bae YC, Jung JS. miR-137 controls proliferation and differentiation of human adipose tissue stromal cells. *Cell Physiol Biochem* 2014; **33**: 758–768.
20 Kim YJ, Hwang SJ, Bae YC, Jung JS. MiR-21 regulates adipogenic differentiation through the modulation of TGF-beta signaling in mesenchymal stem cells derived from human adipose tissue. *Stem Cells* 2009; **27**: 3093–3102.
21 Kim YJ, Bae SW, Yu SS, Bae YC, Jung JS. miR-196a regulates proliferation and osteogenic differentiation in mesenchymal stem cells derived from human adipose tissue. *J Bone Miner Res* 2009; **24**: 816–825.
22 Kim Y, Kim H, Cho H, Bae Y, Suh K, Jung J. Direct comparison of human mesenchymal stem cells derived from adipose tissues and bone marrow in mediating neovascularization in response to vascular ischemia. *Cell Physiol Biochem* 2007; **20**: 867–876.
23 Dweep H, Sticht C, Pandey P, Gretz N.. miRWalk–database: prediction of possible miRNA binding sites by 'walking' the genes of three genomes. *J Biomed Inform* 2011; **44**: 839–847.
24 Annibali D, Gioia U, Savino M, Laneve P, Caffarelli E, Nasi S. A new module in neural differentiation control: two microRNAs upregulated by retinoic acid, miR-9 and -103, target the differentiation inhibitor ID2. *PLoS One* 2012; **7**: e40269.
25 Meyerson M, Enders GH, Wu CL, Su LK, Gorka C, Nelson C *et al.* A family of human cdc2-related protein kinases. *EMBO J* 1992; **11**: 2909–2917.
26 Grossel MJ, Hinds PW.. From cell cycle to differentiation: an expanding role for cdk6. *Cell Cycle* 2006; **5**: 266–270.
27 Kikkawa N, Kinoshita T, Nohata N, Hanazawa T, Yamamoto N, Fukumoto I *et al.* microRNA-504 inhibits cancer cell proliferation via targeting CDK6 in hypopharyngeal squamous cell carcinoma. *Int J Oncol* 2014; **44**: 2085–2092.
28 Moro T, Ogasawara T, Chikuda H, Ikeda T, Ogata N, Maruyama Z *et al.* Inhibition of Cdk6 expression through p38 MAP kinase is involved in differentiation of mouse prechondrocyte ATDC5. *J Cell Physiol* 2005; **204**: 927–933.
29 Zhu X, Li Y, Shen H, Li H, Long L, Hui L *et al.* miR-137 inhibits the proliferation of lung cancer cells by targeting Cdc42 and Cdk6. *FEBS Lett* 2013; **587**: 73–81.
30 Chen L, Holmstrom K, Qiu W, Ditzel N, Shi K, Hokland L *et al.* MicroRNA-34a inhibits osteoblast differentiation and *in vivo* bone formation of human stromal stem cells. *Stem Cells* 2014; **32**: 902–912.
31 Kaneko H, Dridi S, Tarallo V, Gelfand BD, Fowler BJ, Cho WG *et al.* DICER1 deficit induces Alu RNA toxicity in age-related macular degeneration. *Nature* 2011; **471**: 325–330.
32 Luense LJ, Carletti MZ, Christenson LK. Role of Dicer in female fertility. *Trends Endocrinol Metab* 2009; **20**: 265–272.
33 Kanji MS, Martin MG, Bhushan A. Dicer1 is required to repress neuronal fate during endocrine cell maturation. *Diabetes* 2013; **62**: 1602–1611.
34 Oskowitz AZ, Penfornis P, Tucker A, Prockop DJ, Pochampally R. Drosha regulates hMSCs cell cycle progression through a miRNA independent mechanism. *Int J Biochem Cell Biol* 2011; **43**: 1563–1572.
35 Bai Y, Qiu GR, Zhou F, Gong LY, Gao F, Sun KL. Overexpression of DICER1 induced by the upregulation of GATA1 contributes to the proliferation and apoptosis of leukemia cells. *Int J Oncol* 2013; **42**: 1317–1324.
36 Feinberg-Gorenshtein G, Guedj A, Shichrur K, Jeison M, Luria D, Kodman Y *et al.* MiR-192 directly binds and regulates Dicer1 expression in neuroblastoma. *PLoS One* 2013; **8**: e78713.
37 Gaur T, Hussain S, Mudhasani R, Parulkar I, Colby JL, Frederick D *et al.* Dicer inactivation in osteoprogenitor cells compromises fetal survival and bone formation, while excision in differentiated osteoblasts increases bone mass in the adult mouse. *Dev Biol* 2010; **340**: 10–21.
38 Kaneshiro S, Ebina K., Shi K, Higuchi C, Hirao M, Okamoto M *et al.* IL-6 negatively regulates osteoblast differentiation through the SHP2/MEK2 and SHP2/Akt2 pathways *in vitro*. *J Bone Miner Metab* 2014; **32**: 378–392.
39 Suzuki D, Yamada A, Aizawa R, Funato S, Matsumoto T, Suzuki W *et al.* BMP2 differentially regulates the expression of Gremlin1 and Gremlin2, the negative regulators of BMP function, during osteoblast differentiation. *Calcif Tissue Int* 2012; **91**: 88–96.
40 Ahmed FE, Ahmed NC, Vos PW, Bonnerup C, Atkins JN, Casey M *et al.* Diagnostic microRNA markers to screen for sporadic human colon cancer in stool: I. Proof of principle. *Cancer Genomics Proteomics* 2013; **10**: 93–113.
41 Wang X, Guo B, Li Q, Peng J, Yang Z, Wang A *et al.* miR-214 targets ATF4 to inhibit bone formation. *Nat Med* 2013; **19**: 93–100.
42 Zhang YH, Shen L, Shen Y, Chen XD, Jiang LS. Study on key genes and regulatory networks associated with osteoporosis by microarray technology. *Genet Test Mol Biomarkers* 2013; **17**: 625–630.
43 Kim JH, Lee MR, Kim JH, Jee MK, Kang SK. Retraction: 'IFATS collection: selenium induces improvement of stem cell behaviors in human adipose-tissue stromal cells via SAPK/JNK and stemness acting signals'. *Stem Cells* 2013; **31**: 2848.